



ORIGINAL ARTICLE

Removal of ionic liquids and ibuprofen by adsorption on a microporous activated carbon: Kinetics, isotherms, and pore sites



Hanen Guedidi ^{a,b,*}, Imadeddine Lakehal ^a, Laurence Reinert ^a, Jean-Marc Lévêque ^a, Nizar Bellakhal ^b, Laurent Duclaux ^a

^a Univ. Savoie Mont-Blanc, LCME, F-73000 Chambéry, France

^b Laboratoire de Chimie Analytique et Electrochimie, Université de Tunis, 2092 Manar II, Tunisia

Received 2 February 2017; accepted 1 April 2017

Available online 9 April 2017

KEYWORDS

Adsorption;
Kinetics;
Isotherms;
Activated carbon cloth;
Ibuprofen;
Ionic liquid

Abstract Ionic liquids (ILs) are considered as emergent pollutants as their synthesis and further use at a large scale might generate environmental problems. The adsorption on activated carbons represents one of the most effective methods to remove ionic liquids and other micropollutants from wastewater. In this work, the adsorption properties on an activated carbon cloth of two pyridinium ionic liquids (4-tert-butyl-1-propylpyridinium bromide (IL1) and 4-tert-butyl-1-(2-carboxyethyl)pyridinium bromide (IL2)) newly synthesized, were compared with the ones of ibuprofen. The adsorption kinetics and isotherms were studied at pH 3 and 7.5. The adsorption thermodynamic parameters calculated from the isotherms indicate an exothermic process, typical of physisorption. The adsorption kinetics of a mixture of the molecules show a competition between ibuprofen and IL2. The location of each adsorbed ionic liquid and ibuprofen into the porosity of the activated carbon cloth was determined from N₂ (at 77 K) and CO₂ adsorption isotherms (at 273 K). The purification process of an effluent containing the ionic liquids and the ibuprofen in mixture or in single solute could be workable by adsorption on an activated cloth.

© 2017 The Authors. Production and hosting by Elsevier B.V. on behalf of King Saud University. This is an open access article under the CC BY-NC-ND license (<http://creativecommons.org/licenses/by-nc-nd/4.0/>).

1. Introduction

Emerging Organic Contaminants (EOCs) are defined as organic substances present in very small amount in the environment (at concentration levels of nanograms to micrograms per liter), and they are persistent and have potential health effects on organisms or other adverse ecological effects (Stuart and Lapworth, 2013; Mostofa et al., 2012; De la Cruz et al., 2012). Many of them are produced industrially and are dispersed in the environment through domestic, commercial or industrial uses, leading to surface-water, soil and groundwater contamination. EOCs include different families of

* Corresponding author at: Univ. Savoie Mont-Blanc, LCME, F-73000 Chambéry, France.

E-mail address: guedidihanen@yahoo.fr (H. Guedidi).

Peer review under responsibility of King Saud University.



Production and hosting by Elsevier

organic compounds such as pharmaceuticals, personal care products, endocrine-disrupting compounds, steroids and hormones, perfluorinated compounds or ionic liquids (Mostofa et al., 2012). Ibuprofen is one of the pharmaceuticals frequently detected in effluents from sewage-treatment plants at significant concentration, i.e. up to $\sim 25 \text{ mg L}^{-1}$ (Miege et al., 2008). Many studies were devoted to the removal of this molecule from aqueous solutions, as for example by adsorption on activated carbons (Mestre et al., 2007; Baccar et al., 2012). Previous studies pointed out that the presence of carbonyl, lactonic and carboxylic groups on the surface of a microporous-mesoporous activated carbon enhanced its adsorption capacities of ibuprofen whereas the presence of phenolic groups decreased it (Guedidi et al., 2013, 2017). Very recently, Mukoko et al. have prepared an activated carbon from rice hull and proved its efficiency for the removal aspirin, paracetamol and ibuprofen contained in hospital effluents (Mukoko et al., 2015). The studies showed that these contaminants can be removed from wastewater using activated carbon.

Ionic liquids (ILs) constitute a very recent class of EOCs. These organic salts having a large number of molecular structures possess low melting points (below 373 K) and negligible vapor pressure. Since many of them are water soluble and poorly biodegradable, their increasing use might have a harmful impact on the environment (Pham et al., 2010). Even so, their excellent physical properties make them useful in synthesis and catalysis (Liu et al., 2009; Welton, 2004), electrochemistry (Stepniak et al., 2014), solar cells (Xu et al., 2013) or depollution. Various methods, such as thermal degradation (Awad et al., 2004), advanced oxidation processes (Stepnowski and Zaleska, 2005) or biological treatments (Romero et al., 2008) were recently used to remove ILs from wastewater. These techniques are however destructive and do not allow the recovery of the ionic liquids.

An alternative for their uptake is the adsorption onto solids. Several previous studies have concerned the adsorption of ionic liquids from aqueous solutions on activated carbons having various oxygenated surface groups (Farooq et al., 2012; Hassan et al., 2014; Palomar et al., 2009). Palomar et al. (2009) studied the adsorption of imidazolium-based ILs by a commercial microporous activated carbon whose surface was oxidized by various chemical treatments. They demonstrated that the adsorption of hydrophilic ILs was enhanced after oxidation, due to an increase in the amount of oxygenated surface groups promoting hydrogen-bonding interactions between the IL and the adsorbent. In another study, Lemus et al. (2012) showed that activated carbons with low concentration of polar surface groups (obtained by heating treatments at 900°C under N_2) were good adsorbents for hydrophobic ILs and that both the cation and the anion of the IL influenced the adsorption process. They showed that the adsorption was governed by Van der Waals interactions between the alkyl chain linked to the aromatic IL cation and the graphene layers of the activated carbon.

The treatment of pharmaceuticals in wastewater from hospital effluents is also of great concern as some studies indicate that biological treatments are not able to completely remove the micropollutants (Chonova et al., 2016). An additional treatment is thus necessary. The adsorption on activated carbons is one of the most frequently methods used to remove the remaining micropollutants due to a satisfying efficiency compared to other methods for example ozonation (Margot et al., 2013). Compared to granular and powdered activated carbons, activated carbon cloths exhibit rapid adsorption kinetics (Masson et al., 2016; Brasquet et al., 1996; Leyva-Ramos et al., 2012) and high adsorption capacities due to their slit micropores appropriate for the adsorption of small organic molecules (Guedidi et al., 2013, 2017).

To the best of our knowledge, no work about the removal of ionic liquids from wastewater was published, probably because these compounds are not industrially used yet. However, in future time, effluents containing both pharmaceutical and ionic liquids might be produced and efficient treatments will be required to prevent their release in the environment.

The aim of this study was to evaluate the adsorption properties of an activated carbon cloth toward ibuprofen and two novel ionic liquids: the 4-tert-butyl-1-propylpyridinium bromide and the 4-tert-butyl-1-(2-carboxyethyl)pyridinium bromide. These ionic liquids were chosen because of their quite similar molecular size than ibuprofen, and also because of the presence of a carboxylic group for one of them, like for ibuprofen. The adsorption kinetics were studied at 298 K and correlated with the adsorbate's characteristics. Thermodynamic parameters of adsorption were determined from the adsorption isotherms of each molecule studied at different temperatures. Adsorption kinetics of a mixture of the three molecules was also investigated.

2. Experimental

2.1. Adsorbate molecules

4-Tert-butyl-1-propylpyridinium bromide (named IL1, Fig. 1a) and 4-tert-butyl-1-(2-carboxyethyl)pyridinium bromide (named IL2, Fig. 1b) were synthesized in our laboratory by conventional methods. Stoichiometric amounts of 4-tert-butylpyridine (96%, Aldrich) and 1-bromopropane (99%, Aldrich) or 3-bromopropionic acid (>99%, Aldrich) were mixed under stirring (24 h, room temperature) in order to get about 25 g of IL1 or IL2, respectively. Reaction products were washed 5 times with ethyl acetate (>99.7%, Aldrich) and further dried under vacuum at 10^{-3} mbar. The final white powders obtained were stored in stoppered flasks under an argon atmosphere placed in a desiccator containing silica gel.

The purities of the synthesized ILs were examined by ^1H and ^{13}C NMR spectroscopy using a Bruker 400 MHz spectrometer after dissolution in CDCl_3 . Chemical shifts were reported to internal TMS and set at 0 ppm. A pK_a of 4.1 was determined for IL2 by volumetric titration.

2-[4-(2-methylpropyl) phenyl]propanoic acid, also named ibuprofen (IBP, Fig. 1c), was purchased from Sigma-Aldrich (>98% purity, $\text{pK}_a = 4.91$). As IBP is very slightly soluble in pure water ($\sim 21 \text{ mg L}^{-1}$) (Yalkowsky and Dannenfelser, 1992), it was dissolved in a $\text{KH}_2\text{PO}_4/\text{Na}_2\text{HPO}_4$ buffer ($\text{pH} = 7.5$). A solubility of 300 mg L^{-1} was determined in this buffered solution. To measure it, an excess of IBP was added to the buffer solution and stirred until dissolution equilibrium was reached. After filtration of the residual undissolved IBP, the concentration of the solution was determined by UV-visible absorption ($\lambda = 220 \text{ nm}$) using a calibration curve obtained from IBP solutions prepared in a 10v/90v methanol/water solvent (Garzon and Martinez, 2004).

The molecular volumes of the adsorbates, determined using Turbomole software (Ahlrichs et al., 1989), were of 0.53 nm^3 for IBP, 2.02 nm^3 for IL1 and 2.27 nm^3 for IL2.

The octanol/water partition coefficient values of IBP, IL1 and IL2 calculated by using Chemsketch software and model of ref. (Viswanadhan et al., 1989) are 3.72, -1.84 and -2.7 , respectively. Thus, IL1 and IL2 are hydrophilic whereas IBP is hydrophobic. Owing to the presence of carboxylic group on IL2, it is more hydrophilic than IL1.

2.2. Activated carbon

The raw activated carbon cloth (ref. 900-20) referred to T0 was provided by Kuraray Chemical Co. Ltd. (Japan). Before adsorption experiments, it was washed with a 0.1 mol L^{-1} hydrochloric acid solution under stirring for 24 h, in order to

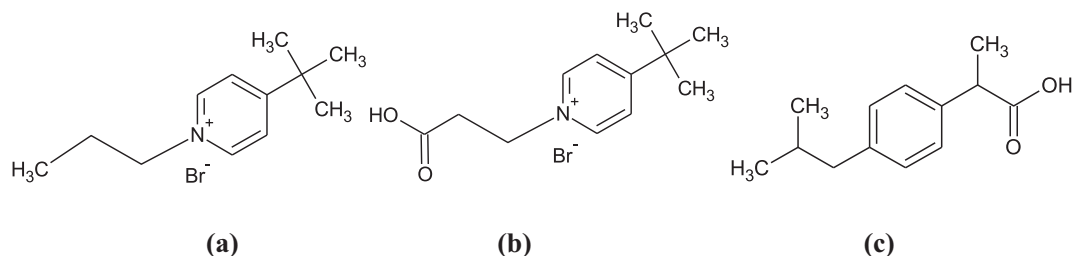


Figure 1 Developed formulas of (a): 4-tert-butyl-1-propylpyridinium bromide (IL1), (b): 4-tert-butyl-1-(2-carboxyethyl)pyridinium bromide (IL2) and (c): ibuprofen.

remove the metal salt impurities. After filtration, it was rinsed with distilled water (~200 mL per g) until reaching a constant pH of the filtrate and dried (383 K, 24 h).

2.3. Textural characterization of the activated carbon cloth before and after adsorption

The porosities of T0 samples prior to and after adsorption were characterized by N_2 adsorption–desorption at 77 K and CO_2 adsorption at 273 K using an ASAP 2020 sorptometer (Micromeritics). The analyzed samples, recovered from the ILs or IBP adsorption isotherm studies, correspond to T0 loaded with the following adsorbate content: 56.7 mg g^{-1} for IBP (Guedidi et al., 2017), 163.82 mg g^{-1} for IL1 and 212.15 mg g^{-1} for IL2. Loaded samples were respectively named T0(IBP), T0(IL1) and T0(IL2). Prior to N_2 or CO_2 adsorption, samples were outgassed for 4 days under vacuum (10^{-3} mmHg) at 323 K. In such conditions, the decomposition of the adsorbed molecules is avoided (Lerdkanhanaporn and Dollimore, 2000).

The specific surface areas of the activated carbons were calculated using the Brunauer–Emmett–Teller (BET) equation, assuming the area of the N_2 molecule to be 0.162 nm². The micropore and mesopore volumes were calculated from the pore size distributions (PSD) of the activated carbons determined using NLDFT (nonlocal density functional theory) models applied on both the adsorption isotherms of N_2 at 77 K and CO_2 at 273 K. For that, infinite slit pores were assumed for CO_2 adsorption (pore diameters from 0.35 to 0.8 nm), while finite slit pores having a diameter-to-width aspect ratio of 12 were used for N_2 adsorption simulations (pore diameters from ~0.45 to 25 nm) (Jagiello and Olivier, 2009). N_2 adsorption data at $P/P_0 < 0.01$ were obtained using incremental fixed doses of 10 cm³ g^{-1} (STP), setting the equilibration interval at 300 s. CO_2 adsorption data were obtained at P/P_0 ranging from 4×10^{-4} to 3.5×10^{-2} , using 45 s equilibration interval (Jagiello and Thommes, 2004).

2.4. Adsorption kinetics and isotherms

The adsorption kinetics of the ILs were studied at room temperature at pH 3 and 7.5. The pH of 3 was adjusted by adding 0.1 mol L^{-1} HCl to the ILs solutions prepared at 0.75 mmol L^{-1} in Ultra High Quality water (UHQ, 18.2 M Ω). Experiments at pH 7.5 were performed by dissolving ILs in a phosphate buffer (prepared by dissolving

1.1796 g of KH_2PO_4 and 4.304 g of Na_2HPO_4 in 1L of UHQ water) (Weast et al., 1990).

Samples of activated carbon cloth (10 mg) were cut off and immersed in flasks containing 10 mL of acidified UHQ water (pH 3) or the buffer solution (pH 7.5). Closed flasks were stirred for at least one hour at 250 rpm in an orbital shaker (New Brunswick Scientific, Innova 40) in order to assure complete wetting of the adsorbent. After this preliminary step, 20 mL of the 0.75 mmol L^{-1} IL solution was added to each flask to obtain an initial concentration of 0.50 mmol L^{-1} . For the kinetics the contact time was set between 2 min and 72 h.

The adsorption isotherms of both ILs and IBP were performed at pH 3 and 7.5 at three different temperatures (286 K, 298 K, and 313 K). 10 mg of the activated carbon cloth was previously impregnated with the solvent as described above. Solutions of given concentrations (from 0.05 to 0.5 mmol L^{-1}), derived from the mother solutions by dilution (with UHQ water for pH 3 or phosphate buffer for pH 7.5) were then added to the flasks and kept under stirring for 24 h.

The adsorption kinetics of a mixture of IBP, IL1 and IL2 were also studied on T0. A disk of T0 (10 mg) was placed in a phosphate buffered aqueous solution (pH 7.5, 298 K, 250 rpm) containing 0.4 mmol L^{-1} of each adsorbate.

All the initial and residual adsorbent concentrations were measured by high performance liquid chromatography (HPLC) using a Waters chromatograph equipped with a high pressure pump (Waters 515), a photodiode array detector (Waters 996) and a Sunfire C18 column (5 μ m, 4.6 \times 250 mm). For IBP analysis, a methanol/UHQ water solution (80/20, v/v), containing 0.1 vol.% of concentrated phosphoric acid (H_3PO_4 , 95 wt.%) in isocratic mode at a flow rate of 1 mL min^{-1} was used as mobile phase. The ILs were analyzed in the same mode using a mobile phase composed either of 88 vol.% of acidified UHQ water and 12 vol.% of methanol for IL1 (1 vol.% of 95 wt.% H_3PO_4 added to the total volume), or of 85 vol.% of acidified UHQ water and 15 vol.% of methanol for IL2. Detection was operated at 220 nm for the IBP and 222 nm for the ILs.

The equilibrium uptake of each molecule Q_{ads} (mg g^{-1}) was calculated from equation:

$$Q_{ads} = \frac{(C_i - C_e) \cdot V}{m}$$

where V is the solution volume (L), C_i and C_e are respectively the initial and equilibrium concentrations of the adsorbent (mmol L^{-1}) and m is the mass of the dry activated carbon cloth (mg).

3. Results and discussion

3.1. Characterization of the activated carbon cloth

The surface chemistry of the activated carbon cloth T0 was characterized by Boehm titration and the determination of pH and pHPzc. The result of Boehm titrations obtained in a previous study (Guedidi et al., 2017) revealed that T0 was mainly acidic with a pH (measured in boiled UHQ water) of 6.05. The basic value of pHPzc (point of zero charge) 8.40 might be assigned to the presence of high content of carbonyl groups (3.45×10^{-4}) on its surface, as confirmed by Boehm titration (Table 1) (Guedidi et al., 2017). The porosity of the activated carbon cloth T0 was characterized by N₂ adsorption-desorption at 77 K and CO₂ adsorption at 273 K. As described in a previous study (Guedidi et al., 2017), the nitrogen adsorption isotherm is of type I and typical of microporous materials according to IUPAC classification (Fig. 2). The isotherm profile is characteristic of narrow microporous sample. As negative unrealistic C factors were obtained by applying the BET model in the 0.05–0.3 relative pressure range, the BET specific surface areas were then preferentially computed in the 0.01–0.05 relative pressure range, as for microporous materials. It is equal to $1910 \text{ m}^2 \text{ g}^{-1}$. The pore size distribution (PSD) of T0 obtained by using a simulation method by NLDFT (Nonlocal density functional theory) model applied on the N₂ adsorption isotherm of T0 at 77 K (Fig. 7) confirms that T0 is mainly microporous in nature: the microporous volume is equal to $0.75 \text{ cm}^3 \text{ g}^{-1}$ whereas the mesoporous volume is only of $\sim 0.04 \text{ cm}^3 \text{ g}^{-1}$. As shown in our previous study, T0 contains two kinds of microporous: The amounts of ultramicropores ($\varnothing < 0.7 \text{ nm}$) and supermicropores ($0.7 < \varnothing < 2 \text{ nm}$) determined by CO₂ and N₂ adsorption respectively (Guedidi et al., 2017) are roughly the same, i.e. of $\sim 0.31 \text{ cm}^3 \text{ g}^{-1}$.

3.2. Chemical characterization of the ionic liquids

The ¹H NMR spectrum of IL1 exhibited peaks at the following chemical shift values from the TMS signal: 9.6 ppm (d, 2H, $J = 7.6 \text{ Hz}$), 8.0 ppm (d, 2H, $J = 7.2 \text{ Hz}$), 4.9 ppm (t, 2H, $J = 7.4 \text{ Hz}$), 2.1 ppm (m, 2H), 1.4 ppm (m, 9H), 1.0 ppm (t, 3H, $J = 6 \text{ Hz}$). A peak of very low intensity observed at 7.23 ppm was assigned to the presence of residual traces of CHCl₃ present in CDCl₃ (Gerotheranassis et al., 2002). The ¹³C NMR spectrum of IL1 showed as expected 8 signals at the following chemical shifts: 145 ppm (2CH), 171.4 ppm (C), 124.7 ppm (2CH), 60.3 ppm (CH₂), 34.2 ppm (C), 25.6 ppm (CH₂), 31.3 ppm (3CH₃) and 11.1 ppm (CH₃).

The ¹H NMR spectrum of IL2 showed peaks at the following chemical shift values from the TMS signal: 9.4 ppm (d, 2H, $J = 6.8 \text{ Hz}$), 8.0 ppm (d, 2H, $J = 7.2 \text{ Hz}$), 5.1 ppm (t, 2H, $J = 6.4 \text{ Hz}$), 3.3 ppm (t, 2H, $J = 6.4 \text{ Hz}$), 1.4 ppm (m, 9H). A very low intensity signal at 7.23 ppm attributed to CHCl₃ was also observed on the IL2 spectrum. The absence of the expected singlet at $\sim 11 \text{ ppm}$ that would confirm the presence of the carboxylic group can be explained by a quick exchange between the acidic proton and a deuterium from the CDCl₃ solvent. The ¹³C NMR spectrum of IL2 exhibited 8 peaks at the following chemical shifts: 171.9 ppm (C), 171.4 ppm (C), 145 ppm (2CH), 124.7 ppm (2CH), 50.3 ppm (C), 34.4 ppm (CH₂), 34.2 ppm (C) and 31.3 ppm (3CH₃).

The ¹H NMR and ¹³C NMR analyses have confirmed the structures and the sufficient purities of IL1 and IL2 (Williams and Fleming, 2007).

3.3. Adsorption kinetics of IL1 and IL2 on T0: effect of pH

The adsorption kinetic of IL1 is faster at pH 3 than at pH 7.5 (Fig. 3). Indeed, the time to reach equilibrium is of about 600 min and 900 min at pH 3 and pH 7.5 respectively. More-

Carboxylic groups	Lactonic groups	Phenolic groups	Carbonyl groups	Total oxygenated groups	Total basic groups	pH	pHP _{ZC}
0.21	0.62	0.1	3.45	4.39	2.25	6.05	8.40

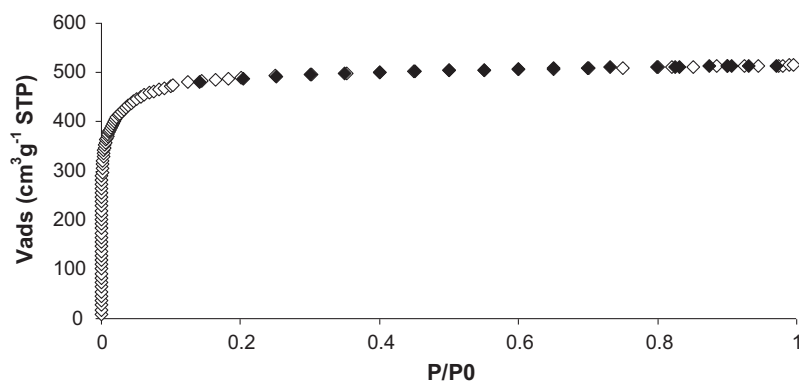


Figure 2 N₂ adsorption-desorption isotherms at 77 K of T0 (◇: adsorption, ◆: desorption).

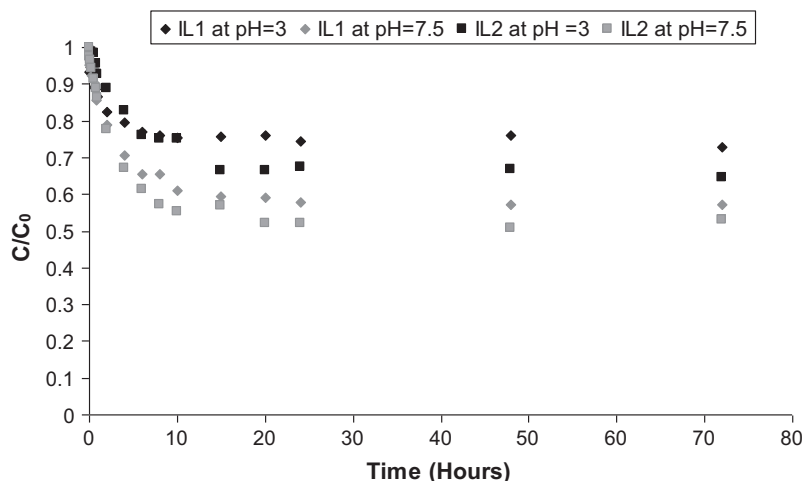


Figure 3 Adsorption kinetics of IL1, IL2 on T0 at pH 3 and 7.5 (298 K, [IL] = 0.5 mmol L⁻¹, mT0 = 10 mg, V = 30 mL, 250 rpm).

over, the IL1 uptake is increased as the pH increases: it is of about 0.37 mmol g⁻¹ at pH 3 compared to 0.65 mmol g⁻¹ at pH 7.5. The adsorption decrease at acidic pH could be explained by a positively charged activated carbon surface (pH < pHPZC) repelling the ionic liquid cation. The adsorption of the IL1 cation at low pH has been only promoted by dispersive interactions. As the pH of the solution has increased, the surface charges of the adsorbent have been neutralized and the adsorption of the ionic cation has consequently increased due to the reduction in the repulsive interaction.

For the IL2 adsorption, the time required to reach adsorption equilibrium is significantly the same at pH 3 and 7.5, i.e. about 900 min (Fig. 3). As for IL1, the activated carbon cloth adsorbed a greater amount of IL2 at pH 7.5 than at pH 3 (~0.5 mmol g⁻¹ and 0.7 mmol g⁻¹ were adsorbed at pH 3 and 7.5 respectively). The lowest adsorption at acidic pH could be explained by repulsive interactions between the positively charged adsorbent and adsorbate (pKa IL2 = 4.1; pH < pKa IL2 < pHPZC). On the other hand, at pH 7.5, the surface of T0 remained positively charged (pH < pHPZC) but IL2 was present under a zwitterionic form due to the deprotonation of the carboxylic acid function. At this pH, the higher adsorption capacity of the activated carbon could be explained by both the electrostatic attractions (between the carboxylate function of IL2 and the positive charges present on the carbon surface) and some π – π dispersive interactions (between the pyridinium ion and the aromatic layers of T0). In a previous study on the adsorption of IBP in a methanol/water (10%v/90%v) solution by the T0 activated carbon cloth, a decrease in the IBP adsorption was observed as increasing pH (Guedidi et al., 2017). Maximum uptakes are about 2.4 mmol g⁻¹ and 0.87 mmol g⁻¹ at pH 3 and 7, respectively (for IBP initial concentration of 100 ppm) and higher than for ILs. Times to reach IBP adsorption equilibrium are of the same order as for the ILs, i.e., about 600 min at pH 3 and 1400 min at pH 7. In comparison with the ILs, the IBP adsorption is promoted at acidic pH because of its strongest hydrophobic nature in relation to its highest K_{ow} (octanol/water partition coefficient) value compared to IL1 and IL2 (Section 2.1). This suggests that at acidic pH, IBP adsorption is mainly governed by hydrophobe-hydrophobe and dispersive interactions between the non-dissociated mole-

cule and the positively charged activated carbon, whereas at pH 7, the hydrophobe-hydrophobe interaction decreases as IBP is dissociated and it is dominant with respect to the electrostatic attractions.

The kinetics of adsorption of the two ionic liquids by T0 was investigated by four models, namely the Lagergren pseudo-first-order model, the pseudo-second-order model and the Elovich model. Table 5 in the Appendix shows the adsorption kinetic parameters calculated from the kinetic models. For both ILs, whatever the pH value, the Elovich model (Table 5 in Appendix) was not in good agreement with the experimental kinetics. For IL1, the best fits of adsorption kinetics at pH 3 and 7.5 ($R^2 = 0.954$ and 0.978 respectively) were obtained using the pseudo-second-order model. The IL1 uptake increased while the pH increased from 3 to 7.5. The pseudo-second-order constant k_2 obtained at pH = 3 is higher than at pH = 7.5. As a consequence, adsorption kinetics of IL1 is quicker when pH decreases. On the other hand, the pseudo first order model was the best one for fitting IL2 adsorption at pH 3 and 7.5 ($R^2 = 0.989$ and 0.995 respectively). The pseudo first order constant k_1 founded at pH 3 is higher than at pH 7.5 indicating that the adsorption kinetics of IL2 adsorption is quicker when pH decreases.

3.4. Adsorption isotherms

3.4.1. Effect of temperature

Whatever the initial pH value and for both ionic liquids, the adsorption capacity of T0 has decreased as increasing the temperature from 286 K to 313 K (Fig. 4a and b), indicating an exothermic phenomenon. The maximum IL1 uptake is reduced from 0.30 to 0.18 mmol g⁻¹ at pH 3 and from 0.65 to 0.60 mmol.g⁻¹ at pH 7.5 (Fig. 4a). A similar temperature variation is brought out for the adsorption of IL2 decreasing from 0.60 to 0.42 mmol g⁻¹ and from 0.73 to 0.63 mmol g⁻¹ at pH 3 and 7.5, respectively. However, the adsorption has been less influenced by the temperature at pH 7.5 than at pH 3 (Fig. 4a and b), maybe because it has been favored at pH 7.5 compared to pH 3. Indeed, the ILs' uptakes were about two times higher at pH 7.5 than at acidic pH.

The adsorption of IBP on T0 in the buffer solution (pH 7.5) has been also an exothermic phenomenon (Fig. 4c) as the IBP

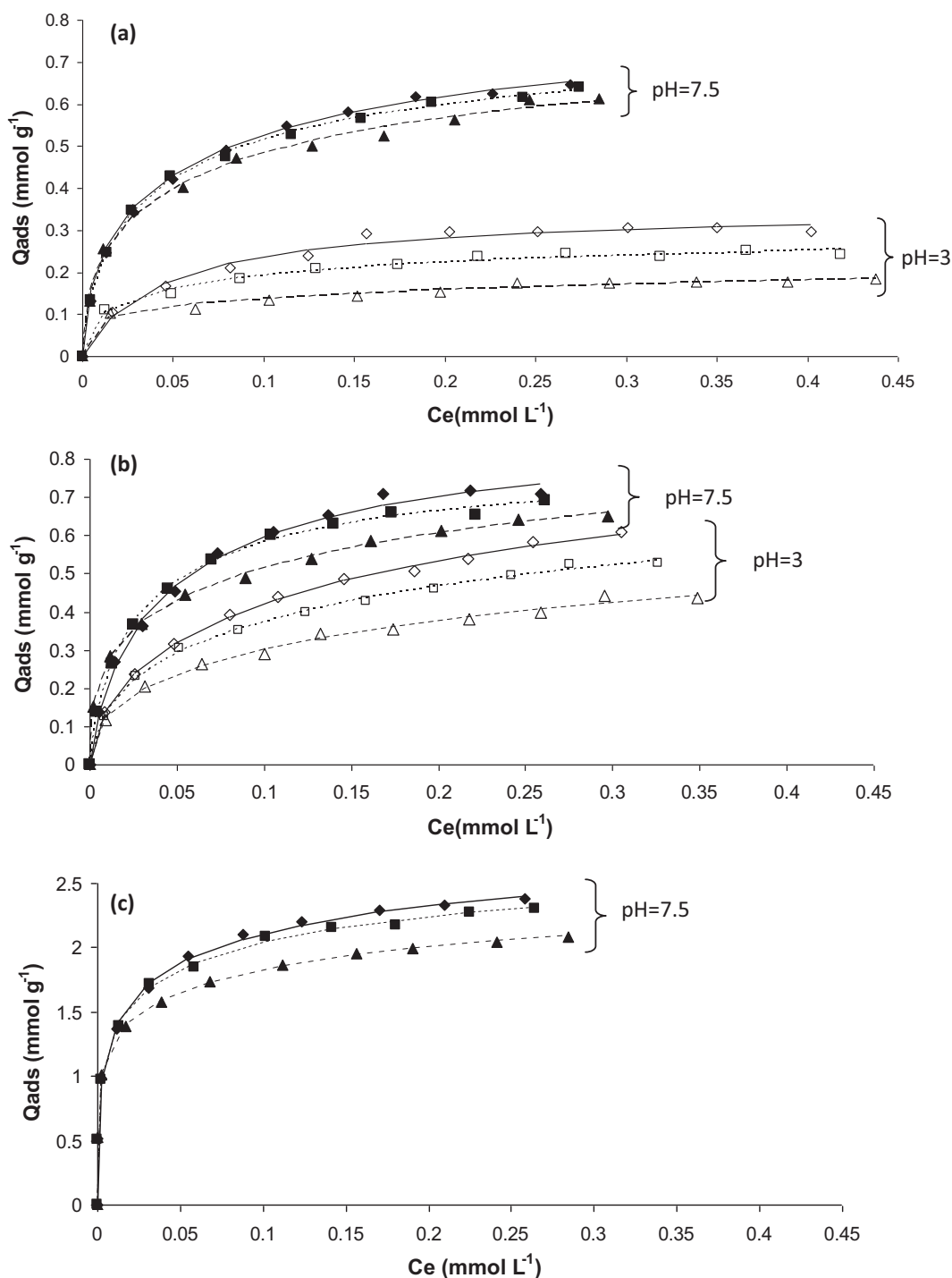


Figure 4 Experimental adsorption isotherms of IL1 (a), IL2 (b) and IBP (c) on T0 at 286 K (◆, ◇), 298 K (■, □) and 313 K (▲, △) fitted by the Langmuir-Freundlich model (lines). Full and empty symbols correspond to isotherms at pH 7.5 and 3, respectively.

uptake has decreased from ~ 2.30 mmol g⁻¹ at 286 K to ~ 2.02 mmol g⁻¹ at 313 K. Exothermal phenomena were also evidenced for the adsorption of IBP from a methanol/water (10%v/90%v) solution on the same activated carbon cloth (T0) (Guedidi et al., 2017) as well as on a microporous-mesoporous granular activated carbon (Guedidi et al., 2013). The exothermic nature of the adsorption phenomenon remains consistent with the solute distribution between the aqueous

phase and the activated carbon as the ILs and IBP solubilities increase together with the temperature. All the adsorption isotherms were tentatively reproduced with the Langmuir (Zhu et al., 2009), Freundlich, Langmuir-Freundlich (Yao, 2000) and Redlich-Peterson (Kumar and Porkodi, 2007) models, using an iterative procedure based on a nonlinear least-squares algorithm (with MATLAB® software).

Whatever the adsorbate and the working pH (Fig. 4), the experimental data were best fitted by the Langmuir-Freundlich model with $R^2 \geq 0.95$ correlation coefficients (in Appendix Tables 6 and 7).

3.4.2. Thermodynamic parameters

Langmuir-Freundlich simulations were used to determine the thermodynamic parameters of adsorption. The Gibbs free energy (ΔG°), enthalpy (ΔH°) and entropy (ΔS°) variations were calculated according to the following equations:

$$\Delta G^\circ = -RT \ln K_d \quad (1)$$

where R ($8.314 \text{ J mol}^{-1} \text{ K}^{-1}$) is the perfect gas constant, T is the solution temperature (K) and K_d is the distribution coefficient. The expression of K_d is as follows:

$$K_d = C_a/C_e \quad (2)$$

where C_a is the IL concentration adsorbed at equilibrium (mmol L^{-1}) and C_e is the concentration of IL remaining in the solution at equilibrium (mmol L^{-1}).

$$\text{Thus, } \ln K_d = -\Delta H^\circ/RT + \Delta S^\circ/R \quad (3)$$

The ΔH° and ΔS° values were calculated from the slope and intercept of the plot of $\ln K_d$ versus $1/T$. Thermodynamic parameters of adsorption of the two ILs were calculated at 298 K, at a constant adsorption uptake value equal to 0.14 mmol g^{-1} at pH 3 and 0.6 mmol g^{-1} at pH 7.5 (Table 2). As uptakes were much higher for IBP, the thermodynamic parameters of adsorption of this latter molecule on T0 at 298 K were calculated at an uptake of 1.21 mmol g^{-1} .

The ΔG° values are negative for all adsorption experiments, implying a spontaneous adsorption of ILs and IBP on T0. Among the two ILs, whatever the pH, the adsorption of IL2 (i.e., 4-tert-butyl-1-(2-carboxyethyl)pyridinium bromide) is the more spontaneous. Thus, the presence of the carboxylic group on IL2 could favor energetically its adsorption with respect to IL1 through hydrogen bonding additional contribution as reported previously by modelizations (Sellaoui et al., 2016) (Table 3). The most negative ΔG° value obtained for the adsorption of IBP (calculated at $Q_{ads} = 1.2 \text{ mmol g}^{-1}$) is attributed to its hydrophobic character. For all the studied systems, the ΔG° values were lower than $\sim 40 \text{ kJ mol}^{-1}$ in agreement with a physisorption process (Yu et al., 2004). These results are in agreement with studies of Farooq et al. (2012) and Hassan et al. (2014) (Table 3) who showed that adsorption of pyridinium ionic liquid onto fabric activated carbon, whatever the pH, was spontaneous and typical of physisorption.

The negative ΔH° values obtained for the ILs and IBP adsorptions (Table 2) are consistent with the decrease in the adsorption capacities as increasing the temperature (Fig. 4a–c) and confirmed that the adsorption is an exothermic process.

The lowest ΔH° value is obtained for the uptake of IL1 at pH 3 ($-37.14 \text{ kJ mol}^{-1}$), and the adsorption process of IL1 on T0 at this pH is therefore the most exothermic and the most energetic. This can be justified by the less spontaneous character of the adsorption of IL1 on T0, thus requiring more energy for this molecule to be adsorbed. Farooq et al. (2012) showed that adsorption of OPyBr by fabric activated carbon tended to be more spontaneous and was found to be less exothermic as the pH increases from 7 to 9 (Table 3).

The negative ΔS° values determined for both ILs at all studied pHs suggest that the adsorption on T0 is accompanied by a disorder decrease: during adsorption, the molecules order themselves on the surface of the activated carbon cloth. The smallest ΔS° value was obtained for the adsorption of IL1 at pH 3 (Table 2, $-124.30 \text{ J K}^{-1} \text{ mol}^{-1}$). This result indicates a more ordered arrangement of IL1 on the surface of T0 compared to the other molecules and it corroborates the most energetic adsorption phenomenon determined for IL1 at pH 3 (see above). It is in agreement with the study published by Farooq et al. (2012) on the adsorption of pyridinium ionic liquids on microporous activated carbons. These authors explained the entropy decrease by the formation of an ordered octylpyridinium monolayer at the surface of the adsorbents (Table 3). Contrary to what is observed for ILs, the ΔS° value for the IBP adsorption on T0 is positive, indicating an increase in disorder. This positive value could indicate a competition between IBP and the molecules from the solvent (phosphate buffered water) to occupy the adsorption sites that would not occur for ILs adsorption.

3.5. Ternary mixture adsorption kinetics of IBP, IL1 and IL2

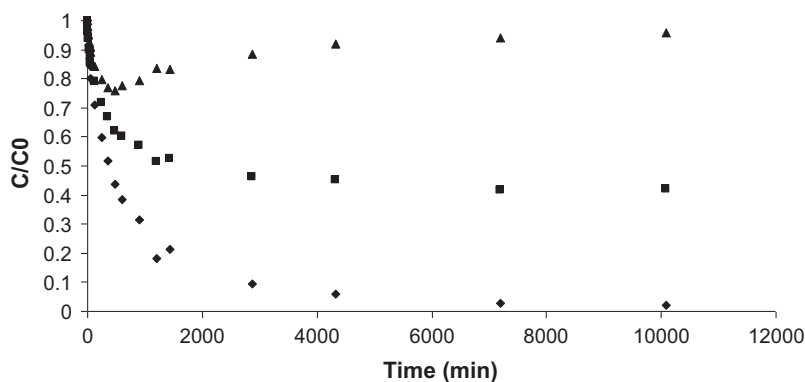
The kinetic curves of the IBP and ILs mixture (pH 7.5, Fig. 5) display that the adsorption equilibrium is achieved much quicker for IL1 and IL2 ($\sim 3000 \text{ min}$) than that for ibuprofen ($\sim 7000 \text{ min}$). Times to reach equilibrium for each molecule of the ternary system are much longer than those previously determined for single adsorption (i.e., $\sim 900 \text{ min}$ for IL1 and IL2). This difference indicates a competitive adsorption between the two ionic liquids and ibuprofen. However, T0 has had a higher affinity for ibuprofen than for both ILs due to its highest hydrophobicity as almost the whole initial amount of IBP has been adsorbed from the ternary mixture against only 60% and 10% of IL1 and IL2, respectively. This is also in agreement with the single-compound experiments for which the maximum adsorption uptakes at pH 7.5 are of about 2.20 mmol g^{-1} for IBP (Fig. 4c) and only around 0.65 mmol g^{-1} for both ILs (Fig. 4a and b). Adsorption behaviors of IL1 and IL2 in the ternary mixture have been quite different. Whereas a continuous decrease in C/C_0 was observed

Table 2 Isothermic Gibbs free energy, enthalpy and entropy variations of the IL1, IL2 and IBP adsorption on T0 (calculated at 298 K).

Adsorbate	IL1	IL1	IL2	IL2	IBP
pH	3	7.5	3	7.5	7.5
Q_{ads} (mmol g^{-1})	0.14	0.60	0.14	0.60	1.21
ΔG° (kJ mol^{-1})	-0.11	-0.20	-3.61	-1.10	-7.06
ΔH° (kJ mol^{-1})	-37.14	-12.19	-11.45	-17.35	-4.06
ΔS° ($\text{J K}^{-1} \text{ mol}^{-1}$)	-124.30	-40.85	-26.32	-59.31	10.04

Table 3 Comparison of results of adsorption of our two pyridinium ILS by T0 and other studies reported in the literature.

AC	ILS	Results	References
AC cloth T0	IL1 IL2	<ul style="list-style-type: none"> – Adsorption of ILS onto T0 was an exothermic process ΔH° (kJ mol⁻¹) = -37.14 (Q_{ads} (mmol g⁻¹) = 0.14 at pH = 3 (IL1)) ΔH° (kJ mol⁻¹) = -12.19 (Q_{ads} (mmol g⁻¹) = 0.60 at pH = 7.5 (IL1)) ΔH° (kJ mol⁻¹) = -11.45 (Q_{ads} (mmol g⁻¹) = 0.14 at pH = 3 (IL2)) ΔH° (kJ mol⁻¹) = -17.35 (Q_{ads} (mmol g⁻¹) = 0.60 at pH = 7.5 (IL2)) – ΔG° values are consistent with a physisorption mechanism ΔG° (kJ mol⁻¹) = -0.11 (Q_{ads} (mmol g⁻¹) = 0.14 at pH = 3 (IL1)) ΔG° (kJ mol⁻¹) = -0.20 (Q_{ads} (mmol g⁻¹) = 0.60 at pH = 7.5 (IL1)) ΔG° (kJ mol⁻¹) = -3.61 (Q_{ads} (mmol g⁻¹) = 0.14 at pH = 3 (IL2)) ΔG° (kJ mol⁻¹) = -1.10 (Q_{ads} (mmol g⁻¹) = 0.60 at pH = 7.5 (IL2)) – ΔS° values indicate an increase in order (Arrangement of ILS) ΔS° (J K⁻¹ mol⁻¹) = -124.30 (Q_{ads} (mmol g⁻¹) = 0.14 at pH = 3 (IL1)) ΔS° (J K⁻¹ mol⁻¹) = -40.85 (Q_{ads} (mmol g⁻¹) = 0.60 at pH = 7.5 (IL1)) ΔS° (J K⁻¹ mol⁻¹) = -26.32 (Q_{ads} (mmol g⁻¹) = 0.14 at pH = 3 (IL2)) ΔS° (J K⁻¹ mol⁻¹) = -59.31 (Q_{ads} (mmol g⁻¹) = 0.60 at pH = 7.5 (IL2)) A physisorption mechanism 	This study
AC cloth T0	IL1 IL2	<ul style="list-style-type: none"> ΔE = -9.07 kJ mol⁻¹ (IL1) ΔE = -10.90 kJ mol⁻¹ (IL2) The adsorption energy values are typical of 	Sellaoui et al. (2016)
Fabric AC	BPyBr	<ul style="list-style-type: none"> ΔH° (kJ mol⁻¹) = -28 ΔG° (kJ mol⁻¹) = -1.3 ΔS° (J K⁻¹ mol⁻¹) = -40.85 (Q_{ads} (mmol g⁻¹) = 0.15 at pH = 7) – Adsorption of ionic liquids onto ACs was exothermic and was typical of physisorption – The entropy value confirmed an increase in order after adsorption due to the local organization of molecule inside the pores 	Hassan et al. (2014)
Microporous-mesoporous AC fabric	OPyBr	<ul style="list-style-type: none"> (Q_{ads} (mmol g⁻¹) = 0.5 at pH = 7) ΔH° (kJ mol⁻¹) = -29.4 ΔG° (kJ mol⁻¹) = -2.8 ΔS° (J K⁻¹ mol⁻¹) = -89 (Q_{ads} (mmol g⁻¹) = 0.5 at pH = 9) ΔH° (kJ mol⁻¹) = 12.7 ΔG° (kJ mol⁻¹) = -5.2 ΔS° (J K⁻¹ mol⁻¹) = 60 – Adsorption tended to be more spontaneous and was found to be less exothermic as the pH increases from 7 to 9 – Adsorption was entropically favored at basic pH 	Farooq et al. (2012)

**Figure 5** Adsorption kinetics of IL1 (■), IL2 (▲) and IBP (◆) from a ternary mixture on T0 (pH 7.5, 298 K, initial concentration of 0.4 mmol L⁻¹ for each molecule, m_{T0} = 10 mg, V = 30 mL, 250 rpm).

for IL1 until the plateau has been reached, IL2 was firstly adsorbed (during the first 500 min) and further desorbed to reach a plateau after about 3000 min. While IL2 was desorbed,

IBP and IL1 continued diffusing toward the activated carbon adsorption sites (Fig. 5). This phenomenon might be related to the adsorbates' molecular sizes which govern their ability to

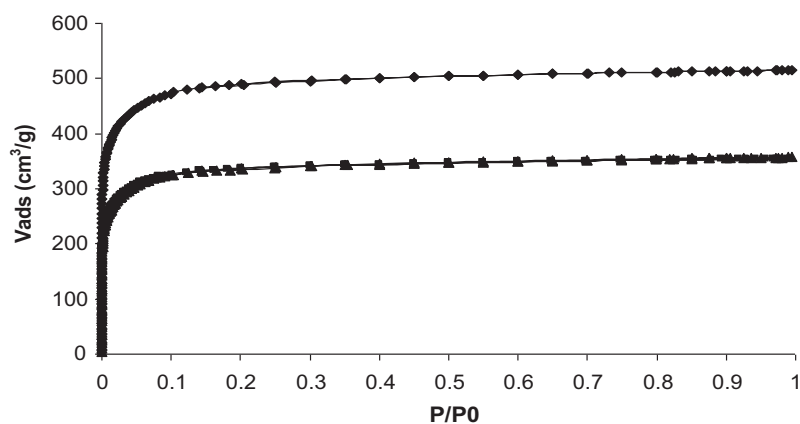


Figure 6 N_2 adsorption-desorption isotherms at 77 K of T0 (◆), T0 (IL1) (▲) and T0(IL2) (■). Curves of T0(IL1) and T0(IL2) are quite superimposed.

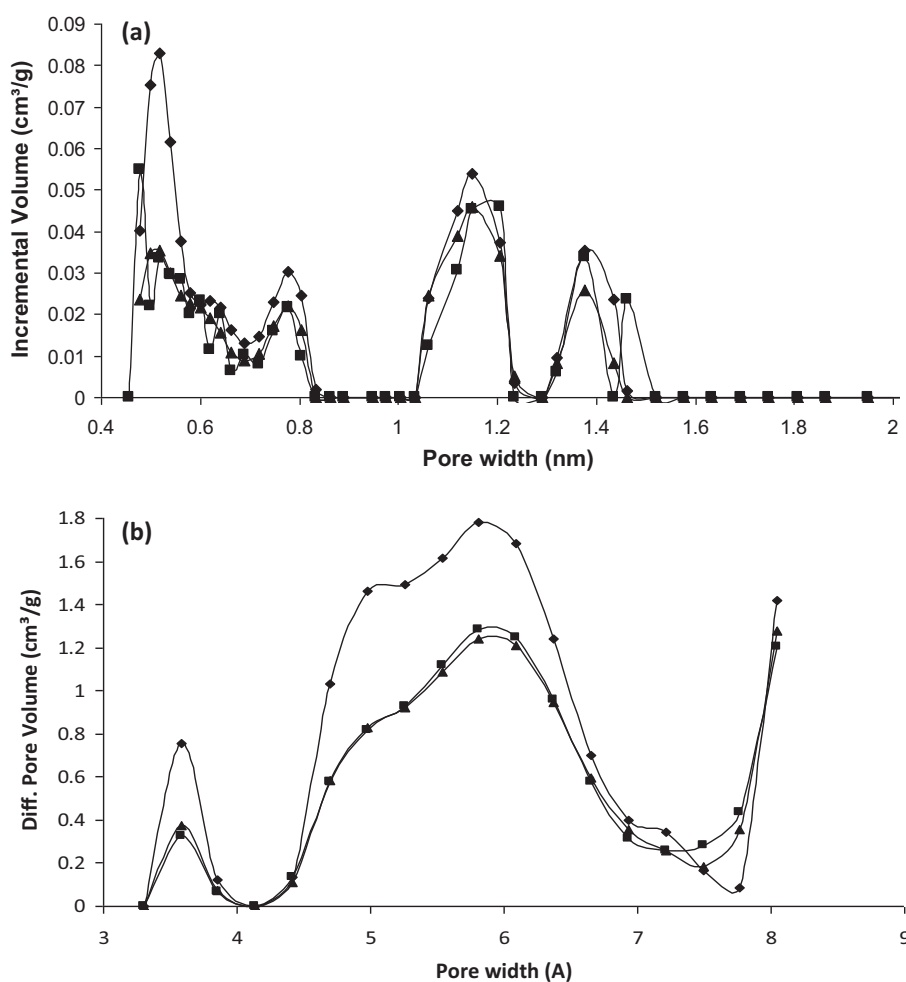


Figure 7 Pore size distributions of T0 (◆), T0(IL1) (▲) and T0(IL2) (■) from DFT simulations by slit-pore models of N_2 (a) and CO_2 (b) isotherms.

diffuse in the porous network of T0. Ibuprofen, which is the smallest molecule (0.53 nm^3), could diffuse much faster in the porosity of T0, which is mainly microporous (Fig. 6), compared to the bulkiest IL1 (2.02 nm^3) and IL2 (2.27 nm^3) mole-

cules. In addition, the lowest affinities of ILs for T0 at pH 7.5 can be explained by the electrostatic repulsions between the positive charge of the ILs cations and the positive surface of T0 ($pH_{PZC} \sim 8.4$) on the one hand, and on the other by the

Table 4 Textural properties of T0 before and after IBP or ILs adsorption, obtained by N₂ adsorption-desorption (77 K) and CO₂ adsorption (273 K). Comparison of the occupied T0 porous volumes calculated from gas adsorption and from the solution adsorption isotherms (Fig. 3) using the molecular volumes.

Sample	T0	T0(IBP)	T0(IL1)	T0(IL2)
S_{BET} (m ² g ⁻¹) ^a	1910	1244	1313	1328
Micropore volume (cm ³ g ⁻¹) ^b	0.750	0.470	0.514	0.503
Ultrapore volume (cm ³ g ⁻¹) ^c	0.310	0.120	0.185	0.185
Supermicropore volume (cm ³ g ⁻¹) ^b	0.320	0.250	0.250	0.253
Ultrapore vol. occupied (cm ³ g ⁻¹) ^d		0.190	0.125	0.125
Supermicropore vol. occupied (cm ³ g ⁻¹) ^d		0.070	0.070	0.068
Occupied volume from isotherms (cm ³ g ⁻¹) ^e		0.200	0.790	0.950

^a Calculated in the 0.01–0.05 P/P^0 range.

^b From N₂ adsorption using aNL-DFT carbon finite slit pore model.

^c From CO₂ adsorption using a DFT carbon infinite slit pore model.

^d Calculated by difference between the porous volumes obtained after and before IBP or ILs adsorption.

^e Calculated with the maximum uptakes from adsorption isotherms and the molecular IBP and ILs volumes.

Table 5 Results of the IL kinetic fittings for T0 sample (pseudo-first order, pseudo-second order and Elovich models).

Kinetic model	Parameters	IL1		IL2	
		pH = 3	pH = 7.5	pH = 3	pH = 7.5
Pseudo-first-order	q_e (mmol g ⁻¹)	0.371	0.621	0.508	0.705
	k_1 (min ⁻¹)	0.034	0.013	0.067	0.012
	R^2	0.925	0.975	0.989	0.995
Pseudo-second-order	q_e (mmol g ⁻¹)	0.394	0.686	0.578	0.780
	k_2 (mmol g ⁻¹ min ⁻¹)	0.056	0.011	0.006	0.009
	R^2	0.954	0.978	0.985	0.990
Elovich	α (mmol g ⁻¹ min ⁻¹)	0.062	0.144	9.487×10^4	9.575×10^5
	β (g mmol ⁻¹)	19.290	8.331	73	50.140
	R^2	0.940	0.938	0.331	0.373

hydrophilic nature of the ILs toward the hydrophobic T0 carbon surface. The presence of a carboxylate group on the IL2 molecule ($pK_a = 4.1$) does not favor its adsorption at equilibrium suggesting that steric dimensions are key parameters for the adsorption. On the contrary, the highest IBP uptake could be justified by both the main contribution of hydrophobic-hydrophobic interactions and the one of the electrostatic attraction between this negatively charged adsorbate ($pK_a = 4.91$) and the positive T0 surface. A recent study (Sellaoui et al., 2016) has demonstrated using the COSMO-RS model that the highest interaction energy of IL2 or IBP with the carbon surface is due to an additional contribution of hydrogen bonds and to the presence of a carboxyl group on these adsorbate molecules. Thus, IL2 and IBP could be adsorbed on similar sites having oxygen surfaces groups through a contribution of hydrogen bonding. This could explain that these adsorbates compete together and that IL2 was desorbed in the ternary kinetics study and mainly replaced by IBP. The strongest hydrophobicity of IBP might be the driving force that has promoted its substitution with IL2 (Fig. 5).

3.6. Pore size required for ILs adsorption

A previous study has demonstrated that the IBP adsorption occurs in both the large ultramicropores and the supermicropores

of the T0 activated carbon cloth (Guedidi et al., 2017). Indeed, gas adsorption experiments have suggested that the ultramicropore volume (0.190 cm³ g⁻¹, representing ~61 vol. %) and supermicropores (0.070 cm³ g⁻¹, representing ~21 vol. %) have been occupied by the IBP molecule (Table 4). Moreover, the occupied volumes deduced from the gas (N₂ and CO₂) adsorption isotherms and the IBP adsorption isotherm at pH 7.5 are quite similar (0.260 cm³ g⁻¹ and 0.200 cm³ g⁻¹, respectively, Table 3). The locations of the ILs molecules in the T0 porous network were investigated by comparing the porous volumes from the N₂ and CO₂ adsorption isotherms of T0 with the volumes occupied by ILs obtained from the loading content ($Q_{\text{ads}} = 0.63$ mmol g⁻¹ for IL1 and 0.73 mmol g⁻¹ for IL2). The N₂ adsorption-desorption isotherms of T0, T0(IL1) and T0(IL2) are all of type I, and typical of microporous materials according to the IUPAC classification (Fig. 6). The N₂-isotherms of the ILs loaded samples match the one of T0 but are shifted toward the lower adsorption volumes. Similar observation can be made for the CO₂ adsorption isotherms (not shown). The measured BET surface area decreased from 1910 m² g⁻¹ for T0 to ~1320 m² g⁻¹ for T0(IL1) or T0(IL2), confirming the presence of the organic molecules in the porosity. A decrease in the total microporous volume from 0.75 cm³ g⁻¹ to ~0.50 cm³ g⁻¹ was also measured after ILs adsorption (Table 4, Figs. 6 and 7a). The comparison of the ultra and supermicropore volumes

before and after ILs' adsorption has allowed calculating the volumes occupied by each IL in the porosity. They were roughly the same for IL1 and IL2 and represented about $0.125 \text{ cm}^3 \text{ g}^{-1}$ of the ultramicropores and $0.07 \text{ cm}^3 \text{ g}^{-1}$ of the supermicropores (Table 4). These values suggest that about 67% and 28% of the ultramicropore and supermicropore volume respectively, are occupied by the ILs (Fig. 7). However, for the two ILs, their occupied volumes calculated from their adsorption isotherms (at pH 7.5) were much higher ($0.790 \text{ cm}^3 \text{ g}^{-1}$ for IL1 and $0.950 \text{ cm}^3 \text{ g}^{-1}$ for IL2) than the microporous occupied volumes determined by gas adsorption ($0.514 \text{ cm}^3 \text{ g}^{-1}$ for IL1 and $0.503 \text{ cm}^3 \text{ g}^{-1}$ for IL2). This difference suggests that the micropores are not completely accessible by these large molecules. Another reason to explain these discrepancies is that the volumes determined for the ILs (2.02 nm^3 for IL1 and 2.27 nm^3 for IL2) were overestimated. ILs might have another configuration inside the pores due to electrostatic and dispersive interactions with the pore walls than the one taken for the calculation of their volume by modelization of the isolated molecules.

Table 6 Different fitting parameters of adsorption isotherms at pH 3.

Model	Parameters	IL1	IL2
Langmuir	Q_m (mmol g^{-1})	0.257	0.581
	k_L (L mmol $^{-1}$)	37.970	21.460
	R^2	0.970	0.983
Freundlich	k_F (mmol $^{1-1/n}$ L $^{1/n}$ g^{-1})	0.315	0.805
	n	4.438	2.896
	R^2	0.984	0.994
Langmuir-Freundlich	Q_m (mmol g^{-1})	0.369	0.983
	K_{LF} (L mmol $^{-1}$)	3.313	2.190
	n	0.480	0.550
	R^2	0.990	0.998
Redlich-Peterson	K_R (L g^{-1})	31.97	36.32
	a_R (L mmol $^{-1}$)	106.50	48.98
	b	0.834	0.750
	R^2	0.988	0.997

Table 7 Different fitting parameters of adsorption isotherms at pH 7.5.

Model	Parameters	IL1	IL2	IBP
Langmuir	Q_m (mmol g^{-1})	0.667	0.737	2.207
	k_L (L mmol $^{-1}$)	39.480	41.300	176.530
	R^2	0.990	0.994	0.926
Freundlich	k_F (mmol $^{1-1/n}$ L $^{1/n}$ g^{-1})	0.979	1.095	1.180
	n	3.306	3.333	5.754
	R^2	0.984	0.974	0.953
Langmuir-Freundlich	Q_m (mmol g^{-1})	0.820	0.829	3.337
	K_{LF} (L mmol $^{-1}$)	8.018	13.820	105.068
	n	0.675	0.768	0.371
	R^2	0.998	0.998	0.957
Redlich-Peterson	K_R (L g^{-1})	47.830	42.620	1649
	a_R (L mmol $^{-1}$)	58.480	50.460	1227.485
	b	0.845	0.900	0.861
	R^2	0.996	0.995	0.956

4. Conclusion

The adsorption kinetics of two ionic liquids: the 4-tert-butyl-1-propylpyridinium bromide and the 4-tert-butyl-1-(2-carboxyethyl)pyridinium bromide are faster than the adsorption kinetic of ibuprofen on the microporous activated carbon cloth T0 (at initial concentration of 0.5 mmol L^{-1}). Time to reach equilibrium is about 1440 min for ibuprofen and ranges between 600 min and 900 min for both ionic liquids. The thermodynamic parameters calculated from adsorption isotherms at three different temperatures allow concluding to a spontaneous and exothermic adsorption mechanism for both ionic liquids. As for the adsorption of ibuprofen, ΔG° values are consistent with a physisorption mechanism ($-7.06 < \Delta G^\circ < -0.11 \text{ kJ mol}^{-1}$). The negative ΔS° values indicate an increase in order due to the arrangement of the molecules while they are adsorbed inside the pores of the activated carbon. The study of the adsorption sites by pore size distribution analyses on loaded samples indicates that all the adsorbates are accommodated in the micropores and mainly in the ultramicropores.

The adsorption of the ionic liquids is strongly dependent on the pH of the solution: the adsorption uptake increases as the pH increases from 3 to 7.5 due to the rise in electrostatic attraction. Adsorption of the ILs could be governed either by dispersive interactions between the aromatic cycle of the ionic liquids and the aromatic layers of T0 (π - π interactions) or by the electrostatic interaction between the organic cation and the carbon surface.

In case of ibuprofen, the main contribution to adsorption is due to hydrophobic repulsions from the solvent which decreases as increase in pH. Hydrogen bonding can additionally contribute to adsorption for the 4-tert-butyl-1-(2-carboxyethyl)pyridinium bromide and ibuprofen.

The adsorption kinetics of a mixture of the three adsorbates at pH 7.5 highlighted a higher affinity of the adsorbent for ibuprofen. This might be directly correlated with the smallest volume of this molecule and to its hydrophobic nature. Indeed, as ibuprofen is the smallest molecule, it can diffuse at higher uptake into the porous network. Moreover, it is the only one negatively charged at pH 7.5 and also the most insoluble and hydrophobic. These properties favor its transfer toward the surface of the positively charged activated carbon cloth and justify its higher uptake compared to the ionic liquids. The 4-tert-butyl-1-(2-carboxyethyl)pyridinium bromide is assumed to be adsorbed on the same site as ibuprofen owing to the presence of the carboxylate function. The competition of these two molecules during the kinetics of the mixture has yielded to the release of this ionic liquid replaced by ibuprofen.

The adsorption of both ionic liquids and ibuprofen is efficient on a microporous activated carbon cloth. The removal of the mixture of ionic liquid and ibuprofen in an effluent purification process will be workable at trace concentrations as no competition is expected to occur between the micropollutants at these concentrations.

Acknowledgments

The “Région Rhône-Alpes” (France) is thankfully acknowledged for the generous MIRA grant attributed to H. Guedidi.

Appendix A

See Tables 5–7.

References

- Ahlich, R., Bär, M., Häser, M., Horn, H., Kölmel, C., 1989. Electronic-structure calculations on workstation computers - the program system TURBOMOLE. *Chem. Phys. Lett.* 162, 165–169.
- Awad, W.H., Gilman, J.W., Nyden, M., Harris, R.H., Sutto, T.E., Callahan, J., Trulove, P.C., DeLong, H.C., Fox, D.M., 2004. Thermal degradation studies of alkyl-imidazolium salts and their application in nanocomposites. *Thermochim. Acta* 409, 3–11.
- Baccar, R., Sarra, M., Bouzid, J., Feki, M., Blanquez, P., 2012. Removal of pharmaceutical compounds by activated carbon prepared from agricultural by-product. *Chem. Eng. J.* 211–212, 310–317.
- Chonova, T., Keck, F., Labanowski, J., Montuelle, B., Rimet, F., Bouchez, A., 2016. Separate treatment of hospital and urban wastewaters: a real scale comparison of effluents and their effect on microbial communities. *Sci. Total Environ.* 542, 965–975.
- De la Cruz, N., Giménez, J., Esplugas, S., Grandjean, D., de Alencastro, L.F., Pulgarín, C., 2012. Degradation of 32 emergent contaminants by UV and neutral photo-Fenton in domestic wastewater effluent previously treated by activated sludge. *Water Res.* 46, 1947–1957.
- Farooq, A., Reinert, L., Lévêque, J.M., Papaiconomou, N., Irfan, N., Duclaux, L., 2012. Adsorption of ionic liquids onto activated carbons: effect of pH and temperature. *Micropor. Mesopor. Mater.* 158, 55–63.
- Garzon, L.C., Martinez, F., 2004. Temperature dependence of solubility for ibuprofen in some organic and aqueous solvents. *J. Solut. Chem.* 33, 1379–1395.
- Gerothanassis, I.P., Troganis, A., Exarchou, V., Barbarossou, K., 2002. Nuclear Magnetic Resonance (NMR) spectroscopy: basic principles and phenomena, and their applications to chemistry, biology and medicine. *Chem. Educ. Res. Pract. Eur.* 3, 229–252.
- Guedidi, H., Reinert, L., Lévêque, J.M., Soneda, Y., Bellakhal, N., Duclaux, L., 2013. The effect of the surface oxidation of activated carbon, the solution pH and the temperature on adsorption of ibuprofen. *Carbon* 54, 432–443.
- Guedidi, H., Reinert, L., Soneda, Y., Bellakhal, N., Duclaux, L., 2017. Adsorption of ibuprofen from aqueous solution on chemically surface-modified activated carbon cloths. *Arab. J. Chem.* 10, S3584–S3594.
- Hassan, S., Duclaux, L., Lévêque, J.M., Reinert, L., Farooq, A., Yasin, T., 2014. Effect of cation type, alkyl chain length, adsorbate size on adsorption kinetics and isotherms of bromide ionic liquids from aqueous solutions onto microporous fabric and granulated activated carbons. *J. Environ. Manage.* 144, 108–117.
- Jagiello, J., Thommes, M., 2004. Comparison of DFT characterization methods based on N₂, Ar, CO₂, and H₂ adsorption applied to carbons with various pore size distributions. *Carbon* 42, 1227–1232.
- Jagiello, J., Olivier, J.P., 2009. A simple two-dimensional NLDFT model of gas adsorption in finite carbon pores. Application to pore structure analysis. *J. Phys. Chem. C* 113, 19382–19385.
- Kumar, K.V., Porkodi, K., 2007. Comments on “adsorption of 4-chlorophenol from aqueous solutions by xad-4 resin: isotherm, kinetic, and thermodynamic analysis”. *J. Hazard. Mater.* 143, 598–599.
- Lemus, J., Palomar, J., Heras, F., Gilarranz, M.A., Rodriguez, J.J., 2012. Developing criteria for the recovery of ionic liquids from aqueous phase by adsorption with activated carbon. *Sep. Purif. Technol.* 97, 11–19.
- Lerdkanchanaporn, S., Dollimore, D., 2000. The evaporation of Ibuprofen from Ibuprofen sarch mixtures using simultaneous TG-DTA. *Thermochim. Acta* 357–358, 71–78.
- Leyva-Ramos, R., Ocampo-Perez, R., Mendoza-Barron, J., 2012. External mass transfer and hindered diffusion of organic compounds in the adsorption on activated carbon cloth. *Chem. Eng. J.* 183, 141–151.
- Liu, J., Li, Z., Chen, J., Xia, C., 2009. Synthesis, properties and catalysis of novel methyl- or ethyl-sulfate-anion-based acidic ionic liquids. *Catal. Commun.* 10, 799–802.
- Margot, J., Kienle, C., Magnet, A., Weil, M., Rossi, L., de Alencastro, L.F., Abegglen, C., Thonney, D., Chèvre, N., Schärer, M., Barry, D.A., 2013. Treatment of micropollutants in municipal wastewater: ozone or powdered activated carbon? *Sci. Total Environ.* 461–462, 480–498.
- Masson, S., Vaulot, C., Reinert, L., Guittonneau, S., Gadiou, R., Duclaux, L., 2016. Thermodynamic study of seven micropollutants adsorption onto an activated carbon cloth: Van't Hoff method, calorimetry, and COSMO-RS simulations. *Environ. Sci. Pollut. Res.* <http://dx.doi.org/10.1007/s11356-016-7614-0H>.
- Mestre, A.S., Pires, J., Nogueira, J.M.F., Carvalho, A.P., 2007. Activated carbons for the adsorption of ibuprofen. *Carbon* 45, 1979–1988.
- Miege, C., Joubert, J.M., Ribeiro, L., Eusebe, M., Coquery, M., 2008. Removal efficiency of pharmaceuticals and personal care products with varying wastewater treatment processes and operating conditions – conception of a database and first results. *Water. Sci. Technol.* 51, 49–56.
- Mostofa, K.M.G., Liu, C.Q., Minakata, D., Wu, F., Vione, D., Mottaleb, A., Yoshioka, T., Sakugawa H., 2012. In: Mostofa, K.M.G., Yoshioka, T., Mottaleb, A., Vione, D. (Eds.), *Photobiogeochemistry of Organic Matter: Principles and Practices in Water Environments*, Springer Science & Business Media, pp. 273–364.
- Mukoko, T., Mupa, M., Guyo, U., Dziike, F., 2015. Preparation of rice hull activated carbon for the removal of selected pharmaceutical waste compounds in hospital effluent. *J. Environ. Anal. Toxicol.* S7. <http://dx.doi.org/10.4172/2161-0525.S7-008>.
- Palomar, J., Lemus, J., Gilarranz, M.A., Rodriguez, J.J., 2009. Adsorption of ionic liquids from aqueous effluents by activated carbon. *Carbon* 47, 1846–1856.
- Pham, T.P.T., Cho, C.W., Yun, Y.S., 2010. Environmental fate and toxicity of ionic liquids: a review. *Water Res.* 44, 352–372.
- Romero, A., Santos, A., Tojo, J., Rodriguez, A., 2008. Toxicity and biodegradability of imidazolium ionic liquids. *J. Hazard. Mater.* 151, 268–273.
- Sellaoui, L., Guedidi, H., Masson, S., Reinert, L., Lévêque, J.M., Knani, S., Ben, Lamine.A., Duclaux, L., 2016. Steric and energetic interpretations of the equilibrium adsorption of two new pyridinium ionic liquids and ibuprofen on a microporous activated carbon cloth: statistical and COSMO-RS models. *Fluid Phase Equilib.* 414, 156–163.
- Stepniak, I., Andrzejewska, E., Dembna, A., Galinski, M., 2014. Characterization and application of N-ethyl-N-propylpiperidiniumbis(trifluoromethanesulfonyl)imide ionic liquid-based gel polymer electrolyte prepared in situ by photopolymerization method in lithium ion batteries. *Electrochim. Acta* 121, 27–33.

- Stepnowski, P., Zaleska, A., 2005. Comparison of different advanced oxidation processes for the degradation of room temperature ionic liquids. *J. Photochem. Photobiol. A: Chem.* 170, 45–50.
- Stuart, M., Lapworth, D., 2013. Emerging Organic Contaminants in Groundwater. British geological survey, Wallingford, pp. 259–284.
- Viswanadhan, V.N., Ghose, A.K., Revankar, G.R., Robins, R.K., 1989. Atomic physicochemical parameters for three dimensional structure directed quantitative structure-activity relationships. 4. Additional parameters for hydrophobic and dispersive interactions and their application for an automated superposition of certain naturally occurring nucleoside antibiotics. *J. Chem. Inf. Comput. Sci.* 29, 163–172.
- Weast, R.C., Lide, D.R., Astle, M.J., Beyer, W.H., 1990, Handbook of Chemistry and Physics, CRC Press, Boca Raton, Floride, pp. D-144–D-146.
- Welton, T., 2004. Ionic liquids in catalysis. *Coord. Chem. Rev.* 248, 2459–2477.
- Williams, D.H., Fleming, I., 2007. Spectroscopic Methods in Organic Chemistry, sixth ed., McGraw-Hill, pp. 304.
- Xu, D., Chen, X., Wang, L., Qiu, L., Zhang, H., Yan, F., 2013. Performance enhancement for high performance dye-sensitized solar cells via using pyridinyl-functionalized ionic liquid type additive. *Electrochim. Acta* 106, 181–186.
- Yalkowsky, S.H., Dannenfelser, R.M., 1992. Aquasol Database of Aqueous Solubility. Version 5, College of Pharmacy, University of Arizona; Tuscon, AZ.
- Yao, C., 2000. Extended and improved Langmuir equation for correlating adsorption equilibrium data. *Sep. Purif. Technol.* 19, 237–242.
- Yu, Y., Zhuang, Y.Y., Wang, Z.H., Qiu, M.Q., 2004. Adsorption of water-soluble dyes onto modified resin. *Chemosphere* 54, 425–430.
- Zhu, S., Yang, N., Zhang, D., 2009. Poly(N, N-dimethylaminoethyl methacrylate) modification of activated carbon for copper ions removal. *Mater. Chem. Phys.* 113, 784–789.